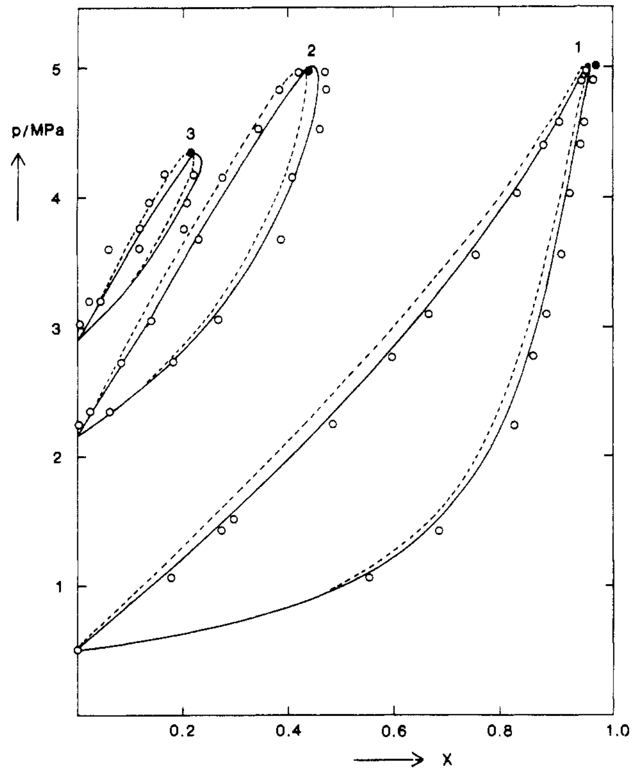

Figure 3. Vapor-liquid equilibria in the system (1 − x)2-methylpropane + $x$ethane, isothermal p,x diagrams: ○, experiments (*2*), ●, experimental critical points (this work); —, calculated by using Peng–Robinson equation (*3*) with $\delta_{ij} = 0$; ----, calculated by using Peng–Robinson equation (*3*) with $\delta_{ij} = 0.031$. 1, 311.26 K, 2, 377.43 K, 3, 394.04 K.

For the Peng-Robinson equation of state the derivatives in eq 1 and 2 are given by Hong et al. (*10*). Evaluation of eq 1 and 2 leads to a set of two equations in three variables T, x, and v. From these equations v and x can be calculated numerically at a given T. The critical pressure can now be calculated from the equation of state.

In Figure 2 the experimental critical curve is compared with the calculated critical points for two values of the binary interaction coefficient δ_{ij} (*3*). For $\delta_{ij} = 0$ one gets an excellent prediction of the p,T projection of the critical curve, but the critical temperature predicted for a given composition can deviate 3.5 K from the experimental critical temperature. For $\delta_{ij} = 0.031$, a value calculated from the experimental critical temperature at $x = 0.5$, the prediction of the T,x projection of the critical curve is very good, but the predicted critical pressures can be 0.1 MPa too low.

Figure 3 shows experimental isothermal phase envelopes at 311.26, 377.43, and 394.04 K and isothermal phase envelopes calculated at these temperatures by using the Peng-Robinson equation with $\delta_{ij} = 0$ and $\delta_{ij} = 0.031$. A value of $\delta_{ij} = 0$ results in a somewhat better overall prediction of the phase envelopes, particularly at lower temperatures.

Registry No. Ethane, 74-84-0; 2-methylpropane, 75-28-5.

Literature Cited

(1) Skripa, V. G.; Nikitina, I. E.; Zhdanovich, L. A.; Sirotin, A. G.; Benyaminovich, O. A. *Gazov. Prom.* **1970**, *15*, 35-36.
(2) Besserer, G. J.; Robinson, D. B. *J. Chem. Eng. Data* **1973**, *18*, 301-304.
(3) Peng, D.; Robinson, D. B. *Ind. Eng. Chem. Fundam.* **1976**, *15*, 59-64.
(4) Loos, Th. W. de; Kool, H. J. van der; Poot, W.; Ott, P. L.; *Delft Prog. Rep.* **1983**, *8*, 200-213.
(5) Redlich, O.; Kister, A. T. *J. Chem. Phys.* **1962**, *36*, 2002-2009.
(6) Deiters, U.; Schneider, G. M.; *Ber. Bunsenges. Phys. Chem.* **1976**, *80*, 1316-1321.
(7) Beegle, B. L.; Modell, M.; Reid, R. C. *AIChE J.* **1974**, *20*, 1200-1206.
(8) Reid, R. C.; Beegle, B. L. *AIChE J.* **1977**, *23*, 726-732.
(9) Gibbs, J. W. "The Scientific Papers"; Dover: New York, 1961; Vol. I, Chapter III.
(10) Hong, G. T.; Modell, M.; Tester, J. W. In "Chemical Engineering at Supercritical Fluid Conditions"; Paulaitis, M. E., Penninger, J. M. L., Gray, R. D., Davidson, P., Eds.; Ann Arbor Science: Ann Arbor, MI, 1983; pp 263-321.

Received for review June 12, 1985. Revised manuscript received September 3, 1985. Accepted September 20, 1985.

Equilibrium Phase Compositions, Phase Densities, and Interfacial Tensions for CO_2 + Hydrocarbon Systems. 2. CO_2 + *n*-Decane

N. Nagarajan and R. L. Robinson, Jr.*

School of Chemical Engineering, Oklahoma State University, Stillwater, Oklahoma 74078

Experimental vapor-liquid equilibrium phase compositions, phase densities, and interfacial tensions are presented for CO_2 + *n*-decane at 160 and 220 °F at pressures to the critical point (interfacial tensions as low as 0.008 mN/m). The phase compositions are in excellent agreement with the data of Reamer and Sage; however, the phase densities exhibit significant differences, with the present data yielding a substantially higher critical-point density. The interfacial tensions represent data not previously available in the literature.

Introduction

The motivation for the work presented here is the need for fundamental data on interfacial tensions (IFT) in CO_2–hydrocarbon systems to serve as the basis for better understanding of the effects of temperature, pressure, and composition on the IFT in such systems. These data could also lead to improved understanding of the process of miscible (or near-miscible, low-IFT) displacement of reservoir oils by CO_2 injection.

The data on CO_2 + *n*-decane presented here is the second in a planned series of studies on CO_2 + hydrocarbon systems which will include measurements on CO_2 with pure and mixed hydrocarbons and on CO_2 with reservoir oils. The first part of this series (*1*) presented data on CO_2 + *n*-butane.

Experimental Method

The apparatus and procedures for the measurements have been described in detail previously (*1*). The only change in procedures employed in the present study involved density

0021-9568/86/1731-0168$01.50/0

Table I. Equilibrium Phase Properties of Pure *n*-Decane

temp, °F	vapor press., psia	phase densities, (kg/m^3) × 10^{-3} liquid	vapor	interfacial tension, mN/m
160	1	0.6887	0.0006	19.20
	(0.4)^a	(0.6901)	(0.0001)	(19.1)
220	2	0.6632	0.0010	16.15
	(1.59)	(0.6620)	(0.0005)	(16.1)

[a] Values in parentheses are from the literature. Vapor pressures and phase densities are by Reamer and Sage (*2*). Interfacial tensions are from Jasper (*3*).

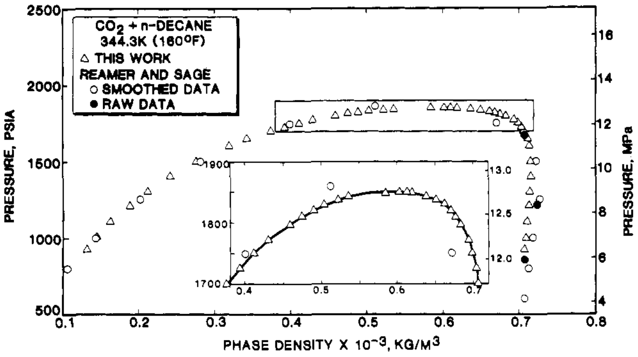

Figure 1. Comparison of phase densities at 160 °F.

measurements. For CO_2 + *n*-butane, the phase densities were measured in a vibrating U-tube densitometer under conditions of flow through the densitometer. For CO_2 + *n*-decane, more stable and reproducible results were obtained when measurements were made when flow through the densitometer was stopped (magnetic circulation pump turned off).

Materials

The CO_2 used in these studies was supplied by Union Carbide Linde Division and had a stated purity of 99.99%. The *n*-decane was from Alpha Products with a stated purity of 99%. These chemicals were used without further purification.

Experimental Results

The complete data appear in Tables I–III. As part of the measurements, the properties of pure *n*-decane were measured. These data appear in Table I, where they are compared to the phase compositions and densities of Reamer and Sage (*2*) and the interfacial tensions of Jasper (*3*). The vapor pressure of decane is less than 2 psia at 160 and 220 °F, and the present apparatus is not designed for such low pressures. However, the measured values are presented for completeness. Measured saturated phase densities agree with those of Reamer and Sage within about $\pm 10^{-3}$ g/cm^3 (kg/m^3 × 10^{-3}). Interfacial tensions for decane differ by less than 1% from the values of Jasper.

Phase densities measured for CO_2 + *n*-decane are illustrated in Figures 1 and 2; also shown are the data of Reamer and Sage (*2*). Agreement of the phase densities is not as good as that found when the CO_2 + *n*-butane data from part 1 of this work (*1*) were compared with the data of Olds et al. (*4*). In general, the present data show lower values for liquid densities at low pressures and higher values as the critical pressure is approached. Values of the critical densities are in marked disagreement (Table III).

An investigation was made to determine the source of the liquid density disagreements. The raw data of Reamer and Sage were reanalyzed, and the results at 160 °F appear in Figure 1. Their smoothed data in the figure (open circles) are based on only three raw data points (closed circles) in the pressure range of the present data. Their highest (1670 psia) and lowest (850 psia) pressure points agree within 0.002 g/cm^3 of our data, while their intermediate pressure point (1210 psia) differs by 0.011 g/cm^3. Thus, including the pure *n*-decane densities from Table I, three of four of their raw data points agree with the present work within 0.002 g/cm^3. This is much better than the agreement shown by their smoothed data. Similar analysis of their data at 220 °F yielded almost identical results.

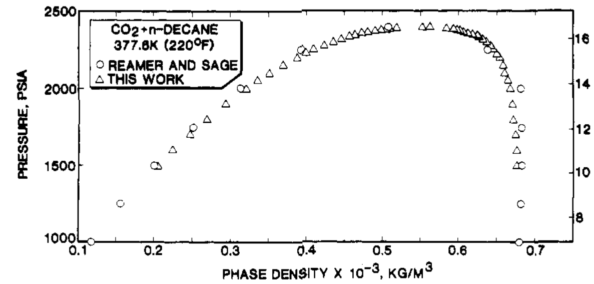

Figure 2. Comparison of phase densities at 220 °F.

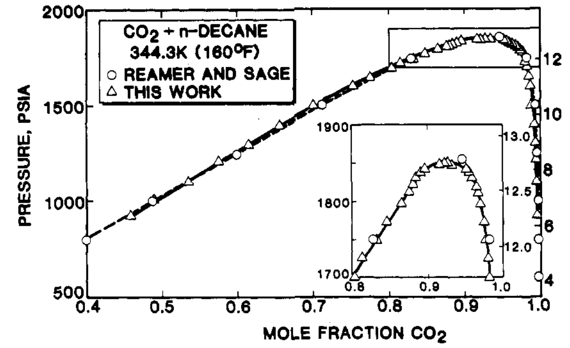

Figure 3. Comparison of phase compositions at 160 °F.

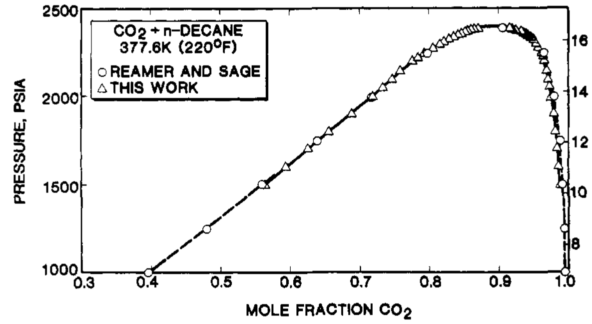

Figure 4. Comparison of phase compositions at 220 °F.

Phase composition data are presented in Figures 3 and 4. Agreement with the data of Reamer and Sage is adequate. Differences are on the order of 0.005 in CO_2 mole fraction, which is probably within the combined uncertainties in the two data sets.

The IFT data from the present work are shown in Figure 5. No literature data are available for this system. The data are shown as a function of the difference in the equilibrium phase densities. This method of presenting the data conveniently expands the low-IFT region; in addition, "scaling laws" require that this relationship becomes linear (log–log) at low IFT values and that the slope is a specific, universal value. (This is discussed further below.)

In the present work (and for the previous CO_2–*n*-butane data), sufficient replicate measurements were made to permit estimation of expected uncertainties in the IFT data. At each pressure, multiple drops were photographed and multiple measurements were made on each photograph. From these

Table II. Phase Equilibria and Interfacial Tensions for Carbon Dioxide + n-Decane

pressure, kPa	pressure, psia	phase compositions, mole fraction CO_2, liquid	phase compositions, mole fraction CO_2, vapor	phase densities, $(kg/m^3) \times 10^{-3}$, liquid	phase densities, $(kg/m^3) \times 10^{-3}$, vapor	interfacial tension, mN/m
			344.3 K (160 °F)			
6385	926	0.457	0.995	0.7081	0.1303	
6940	1007	0.489	0.995	0.7099	0.1456	7.81
7610	1104	0.535	0.995	0.7111	0.1630	6.65
8340	1210	0.575	0.995	0.7140	0.1885	5.67
8960	1300	0.615	0.994	0.7154	0.2119	4.61
9650	1400	0.657	0.993	0.7164	0.2418	3.54
10340	1500	0.702	0.990	0.7166	0.2770	2.53
11020	1599	0.753	0.987	0.7146	0.3194	1.71
11380	1650	0.775	0.986	0.7120	0.3429	1.29
11730	1701	0.804	0.983	0.7074	0.3755	0.848
11900	1726	0.815	0.981	0.7043	0.3930	0.665
12070	1751	0.834	0.979	0.6995	0.4122	0.529
12220	1772	0.847	0.976	0.6944	0.4306	0.356
12400	1799	0.866	0.971	0.6840	0.4595	0.245
12490	1811	0.877	0.968	0.6763	0.4758	0.142
12550	1821	0.883	0.965	0.6708	0.4899	0.101
12620	1830	0.886	0.960	0.6627	0.5039	0.059
12670	1835	0.893	0.955	0.6511	0.5230	0.029
12700	1842	0.897	0.953	0.6379	0.5358	0.0125
12730	1847	0.918	0.935	0.6191	0.5853	
12760[a]	1850	0.925	0.931	0.6128	0.6025	
12740[b]	1848	0.930		0.5905		
			377.6 K (220 °F)			
10340	1500	0.565	0.987	0.6762	0.2051	4.39
11040	1601	0.595	0.985	0.6760	0.2241	3.73
11750	1705	0.626	0.984	0.6742	0.2469	3.08
12420	1801	0.656	0.981	0.6716	0.2688	2.54
13120	1903	0.689	0.978	0.6709	0.2939	1.98
13800	2001	0.719	0.975	0.6677	0.3221	1.42
14150	2053	0.734	0.973	0.6652	0.3366	1.24
14480	2100	0.746	0.970	0.6604	0.3521	0.950
14830	2151	0.757	0.968	0.6587	0.3696	0.792
15170	2201	0.776	0.964	0.6539	0.3886	0.634
15350	2226	0.784	0.962	0.6509	0.3997	0.482
15510	2250	0.794	0.959	0.6472	0.4104	0.390
15690	2276	0.806	0.957	0.6432	0.4241	0.314
15850	2299	0.816	0.953	0.6380	0.4357	0.221
15960	2315	0.821	0.950	0.6336	0.4460	0.171
16070	2331	0.829	0.946	0.6288	0.4573	0.127
16140	2341	0.836	0.944	0.6249	0.4638	0.100
16220	2353	0.842	0.940	0.6195	0.4741	0.069
16280	2362	0.846	0.937	0.6133	0.4814	0.051
16350	2371	0.854	0.933	0.6075	0.4916	0.033
16380	2376	0.856	0.930	0.6027	0.5000	0.020
16410	2381	0.860	0.926	0.5990	0.5061	0.012
16450	2386	0.865	0.922	0.5940	0.5099	0.008
16460	2388	0.870	0.916	0.5845	0.5199	
16490[a]	2392			0.5632	0.5527	
16480[b]	2391	0.895		0.5535		

[a] Suspect data point. [b] Estimated critical point.

Table III. Critical Properties for CO_2 + n-Decane

temp, °F	press., psia	density, $(kg/m^3) \times 10^{-3}$	composition, mole fraction CO_2
160	1848	0.5905	0.930
	(1860)[a]	(0.5120)	(0.948)
220	2391	0.5535	0.895
	(2392)	(0.5074)	(0.905)

[a] Values in parentheses are from Reamer and Sage (2).

measurements, maximum deviations from the mean IFT value were determined. The results appear in Figure 6. The "scatter" in the IFT values for CO_2 + n-decane appears to be consistent with the results for CO_2 + n-butane. The relation

$$\epsilon_\gamma = 0.04\gamma^{0.8} \tag{1}$$

developed from the CO_2 + n-butane data appears to be adequate for the CO_2 + n-decane system also.

Table III presents estimates of the critical-point pressures, compositions, and densities for CO_2 + n-decane at 160 and 220 °F. These values were determined as follows. Scaling-law analysis suggests that

$$\Delta\rho = A_1[(P_c - P)/P_c]^\beta \tag{2}$$

$$\gamma/\Delta\rho = A_2[(P_c - P)/P_c]^{2\nu-\beta} \tag{3}$$

(Note: the pendant drop measurements of IFT actually give values of $\gamma/\Delta\rho$ rather than γ directly.) All data at 160 and 220 °F at pressures within 10% of the critical pressure were analyzed simultaneously in terms of the above two equations. Weighted regressions were performed to determine simultaneously two A_1's, two A_2's, two P_c's, β, and ν. Maximum ex-

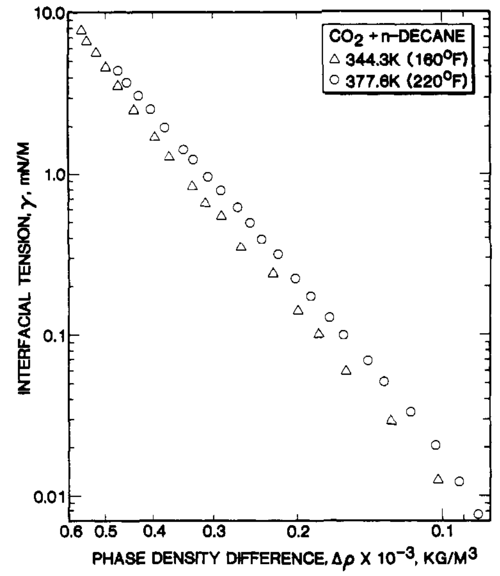

Figure 5. Interfacial tensions for CO_2 + *n*-decane.

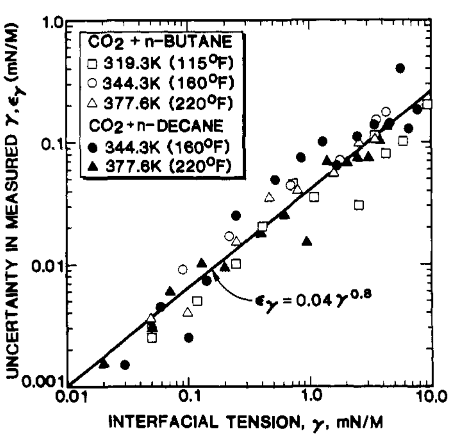

Figure 6. Uncertainties in measured interfacial tensions.

pected uncertainties were assigned to each measured variable as follows:

$$\epsilon_\gamma = 0.04\gamma^{0.8}\ \text{mN/m} \tag{4}$$

$$\epsilon_\rho = 0.0005\ \text{g/cm}^3 \tag{5}$$

$$\epsilon_p = 2\ \text{psi} \tag{6}$$

These values were used to evaluate weighting factors for use in the regressions. The resultant values of P_c are shown in Table III. Values determined for β and ν were 0.368 and 0.646, respectively. These are in adequate agreement with the values of 0.355 ± 0.01 and 0.63 ± 0.02 previously reported for these scaling-law variables (*5*) from analysis of data on pure substance properties. These values are somewhat different from the theoretical values of 0.325 and 0.63 (*6*); the difference may, in part, be due to inclusion of data sufficiently far from the critical point that the asymptotic forms of eq 2 and 3 should be modified to include corrections to scaling. However, the difference is more likely due to experimental uncertainties in the present data. For all data points, the fit to the equation was within the expected maximum uncertainties (estimated from the experimental uncertainties given above). Values of the critical-point densities were determined from "rectilinear diameter" plots of $(\rho^V + \rho^L)/2$ vs. $(P_c - P)$ and critical compositions from plots of $(x + y)/2$ vs. $(P_c - P)$.

In Table II, two data points are denoted as "suspect" since the scaling-law analysis predicts critical pressures below the pressures for these two-phase data points. Measurements very near the critical pressure are quite difficult; the rate of change of $\Delta\rho$ with pressure becomes infinite. Thus, although the two indicated data points are presented in the tables, they appear to be inconsistent with the data at lower pressures.

The IFT data points very near and below γ = 0.01 mN/m are perhaps less accurate than the estimate given by eq 1. The photographic images of the drops become markedly less distinct at pressures near the critical point, apparently due to increased light-scattering behavior of near-critical fluids. This, coupled with the very small diameters (~0.02 cm) of the drops, makes measurements difficult. Values of γ near 0.01 mN/m appear to represent the lower limit of applicability of the present apparatus.

Conclusion

Data are presented for phase compositions, phase densities, and IFT at 160 and 220 °F for the CO_2 + *n*-decane system. The results appear to be of accuracy comparable to the previously reported data on CO_2 + *n*-butane. The IFT data for CO_2 + *n*-decane represent measurements not previously available in the literature. At pressures within 10% of the critical pressure, the data obey asymptotic forms of the scaling relations (eq 2 and 3).

Glossary

A_1, A_2	parameters in eq 2 and 3
P	pressure
P_c	critical pressure
x	liquid-phase mole fraction
y	vapor-phase mole fraction
β, ν	scaling-law parameters (critical indices)
γ	interfacial tension
ϵ_p	uncertainty in measured pressure
ϵ_γ	uncertainty in measured interfacial tension
ϵ_ρ	uncertainty in measured density
ρ^L	liquid-phase density
ρ^V	vapor-phase density
$\Delta\rho$	liquid-phase density minus vapor-phase density

Registry No. CO_2, 124-38-9; decane, 124-18-5.

Literature Cited

(1) Hsu, Jack J.-C.; Nagarajan, N.; Robinson, Jr., R. L. *J. Chem. Eng. Data* **1985**, *30*, 485.
(2) Reamer, H. H.; Sage, B. H. *J. Chem. Eng. Data* **1963**, *8*, 508.
(3) Jasper, J. J. *J. Phys. Chem. Ref. Data* **1972**, *1*, 841.
(4) Olds, R. H.; Reamer, H. H.; Sage, B. H.; Lacey, W. N. *Ind. Eng. Chem.* **1949**, *41*, 475.
(5) Levelt-Sengers, J. M. H.; Greer, W. L.; Sengers, J. V. *J. Phys. Chem. Ref. Data* **1976**, *5*, 1.
(6) Le Guillou, J. C.; Zinn-Justin, J. *Phys. Rev. B* **1980**, *21*, 3976.

Received for review June 13, 1985. Accepted October 10, 1985. Financial support for this work was furnished by the following organizations: Amoco Production Research Co., ARCO Oil and Gas Co., Chevron Oil Field Research Co., Marathon Oil Co., Mobil Research and Development Corp., Shell Development Co., Sun Exploration and Production Co., and Texaco, Inc.